European Journal of Chemistry

View Journal Online
View Article Online

Nitroisatin dithiocarbazate: Synthesis, structural characterization, DFT, and docking studies

Pedro Henrique do Nascimento Pereira [1], Jackelinne Camargo Lima [2], Victor Marcelo Deflon [2], Geoffroy Roger Pointer Malpass [1], Ronaldo Junio de Oliveira [1] and Pedro Ivo da Silva Maia [1,*]

[1] *Núcleo de Desenvolvimento de Compostos Bioativos, Universidade Federal do Triângulo Mineiro, Uberaba-MG, 38064-200, Brazil*
pedrohenriquenasc@hotmail.com (P.H. do N.P.), geoffroy.malpassuftm@gmail.com (G.R.P.M.), ronaldo.oliveira@uftm.edu.br (R.J.O.), pedro.maia@uftm.edu.br (P.I.S.M.)
[2] *Instituto de Química, Universidade de São Paulo, São Paulo-SP, 13560-970, Brazil*
jackelinne_lima@hotmail.com (J.C.L.), deflon@iqsc.usp.br (V.M.D.)

* *Corresponding author at: Núcleo de Desenvolvimento de Compostos Bioativos, Universidade Federal do Triângulo Mineiro, Uberaba-MG, 38064-200, Brazil.*
e-mail: pedro.maia@uftm.edu.br (P.I.S. Maia).

RESEARCH ARTICLE

10.5155/eurjchem.12.3.235-241.2106

Received: 31 January 2021
Received in revised form: 26 March 2021
Accepted: 02 April 2021
Published online: 30 September 2021
Printed: 30 September 2021

KEYWORDS

DFT
Isatins
Dithiocarbazates
Antitumor agents
Molecular docking
Thioredoxin reductase

ABSTRACT

The reaction between 5-nitroisatin with S-benzyl dithiocarbazate affords a new isatindithiocarbazate so-called NO_2Isadtc (Benzyl 2-(5-nitro-2-oxoindolin-3-ylidene)hydrazinecarbodithioate) which was characterized by means of ^{1}H NMR, FT-IR, UV-visible and single crystal X-ray diffraction - Crystal data for $C_{16}H_{12}N_4O_3S_2$ (M =372.42 g/mol): triclinic space group *P*-1, (n°. 02), *a* = 6.640 Å, *b* = 8.256 Å, *c* = 15.908 Å, *V* = 849.6 Å^3, *Z* = 2, T = 293 K, μ(MoK$_\alpha$) = 0.337 mm^{-1}, D_{calc} = 1.456 g/cm^3, 27515 reflections measured (2.499° ≤ 2Θ ≤ 26.524°), 3518 unique (R_{int} = 0.0533, R_{sigma} =0.0222) which were used in all calculations. The final R_1 was 0.0367 (I > 2σ(I)) and wR_2 was 0.1045 (all data). Computational methods were applied to NO_2Isadtc and its nonsubstituted parent compound Isadtc for structure optimization, electronic distribution, and infrared calculations using B3LYP functional with 6-31G(d,p) basis set in ethanol as a polarizable continuum model. Furthermore, docking studies using human thioredoxin reductase 1 (TrxR) as enzyme target also were performed using NO_2Isadtc and the optimized structure of Isadtc. The results demonstrated that both NO_2Isadtc and Isadtc may act as inhibitors of TrxR, having different interactions detected, highlighting the contact between the NO_2 group and the S111 at the helix which is found for NO_2Isadtc.

Cite this: *Eur. J. Chem.* **2021**, *12(3)*, 235-241 **Journal website**: www.eurjchem.com

1. Introduction

Isatin (Figure 1a) is a heterocyclic compound which presents an aromatic ring joined to a second ring formed by ketonic and amidic groups. This configuration allows many modifications in its structure, such as addition of halogen atoms at C5 and C7 positions of the aromatic ring and alkylation/acylation at N-H group which may lead to modifications of its chemical properties [1]. Isatins and their derivatives are known to have a broad spectrum of pharmacological applications such as antifungal, antibacterial, antiviral, antitumor, and antiprotozoal [2-4]. Besides, isatin is a biologically validated as an inhibitor of cysteine and serine proteases [5], being an interesting starting point for the design and synthesis of new compounds with potential for applications in medicine, mainly Schiff bases such as hydrazones, thiosemicarbazones, dithiocarbazates (Figure 1b, 1c and 1d, respectively) and also some of their metal complexes.

Despite of the chemical similarities of thiosemicarbazones and dithiocarbazates [6], few studies involving isatin dithiocarbazates are available in the literature [7-10]. Interestingly, isatin derived thiosemicarbazones were investigated as inhibitors of parasitic cysteine proteases identified in trypanosomes (cruzain and rhodesain) and malaria parasites (falcipain-2), presenting a higher activity than their isatin precursors [2]. On the other hand, dithiocarbazates have been mainly studied as antitumor agents, however, to our knowledge, no studies involving their biological targets have been reported so far.

In this context, the goal of this work was the synthesis and structural characterization of a new isatin dithiocarbazate derived from 5-nitroisatin (NO_2Isadtc). DFT calculations were also applied to both NO_2Isadtc and Isadtc to understand the influence of the NO_2 group on the electronic distribution. Finally, docking studies with human thioredoxin reductase (TrxR) were applied aiming to validate this enzyme as the target

ISSN 2153-2249 (Print) / ISSN 2153-2257 (Online)
https://dx.doi.org/10.5155/eurjchem.12.3.235-241.2106

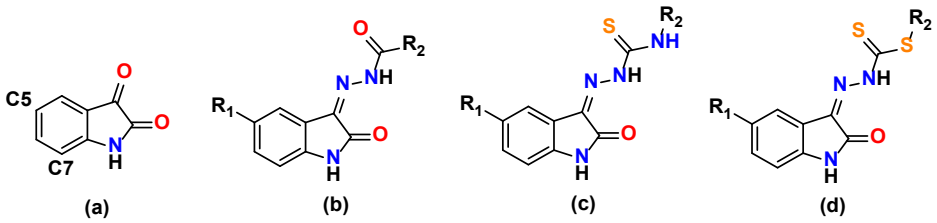

Figure 1. Molecular structure of Isatin (**a**) and its hydrazone (**b**), thiosemicarbazone (**c**) and dithiocarbazate (**d**) derivatives.

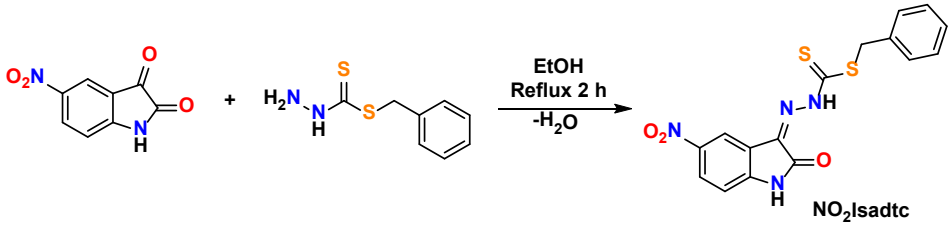

Scheme 1. Synthesis of NO_2Isadtc.

for this class of compounds since it is known to be a representative target for antitumor drug development [9].

2. Experimental

2.1. Materials and physical methods

5-Nitroisatin (Sigma-Aldrich) and all solvents were obtained commercially and used without further purification. S-benzyl dithiocarbazate was synthesized according to a literature procedure [10]. The melting point was determined with a PF1500 FARMA-GEHAKA instrument. Infrared spectra were measured on a Frontier Single Range-MIR PerkinElmer FT-IR spectrophotometer in the region between 220 and 4000 cm^{-1}. Samples were analyzed in the solid state using the Attenuated Total Reflectance (ATR) accessory with diamond crystal. ^1H spectra were acquired in 5 mm NMR tubes at 298 K on a Bruker DPX 400 (^1H = 400.00 MHz) spectrometer. ^1H NMR chemical shifts were internally referenced to DMSO-d_6 (ppm). The electronic spectra were measured in a Shimadzu UV-1800 spectrophotometer at 25 °C using a quartz cuvette of 1 cm optical path.

2.2. Synthesis of NO_2Isadtc

1.5 mmol of 5-nitroisatin (221 mg) and 1.5 mmol of S-benzyl dithiocarbazate (297 mg) were dissolved in 15 mL of ethanol in a round-bottomed flask. The system was warmed under reflux for 2h and a yellow precipitate was formed after cooling to room temperature. The precipitate was filtered off, washed with *n*-hexane and dried under vacuum (Scheme 1).

(Z)-benzyl 2-(5-nitro-2-oxoindolin-3-ylidene)hydrazinecarbodithioate: Color: Bright yellow. Yield: 69%. M.p.: 210-211 °C. FT-IR (KBr, ν, ATR, cm^{-1}): 3595, 3592 ν(N-H), 1715 ν(C=O), 1615 ν(C=N), 1529 ν(C=C), 1336 ν(NO_2), 1064 ν(N-N), 1030 ν(CSS). ^1H RMN (400 MHz, DMSO-d_6, δ, ppm): 4.58 (s, 2H, CH_2), 7.14 (d, J = 8.8 Hz, 1H, isa), 7.31 (t, J = 7.1 Hz, 1H, Ph), 7.36 (t, J = 7.1 Hz, 2H, Ph), 7.47 (d, J = 7.1 Hz, 2H, Ph), 8.21 (d, J = 2.2 Hz, 1H, isa), 8.31 (dd, 3J = 8.6, 4J = 2.2 Hz, 1H, isa), 11.97 (s, 1H, NH), 13.72 (s, 1H, NH). UV/Vis (MeOH, λ_{max}, nm, (ε)): 241 (0.093), 376 (0.558).

2.3. XRD analysis

The X-ray diffraction data were collected on a Bruker APEX-II CCD X-ray diffractometer with Mo Kα (λ = 0.71073 Å) radiation. The structure was solved using SIR92 [11] and refined by full-matrix least-square methods against F^2 with SHELXL2016 [12]. All non-hydrogen atoms were refined with anisotropic displacement parameters with SHELXL2016. The hydrogen atoms' positions were calculated at idealized positions with the "riding model" option of SHELXL2016. Details of the structure refinement and experimental details can be found in Table 1.

2.4. Computational methods

2.4.1. DFT calculations

The refined NO_2Isadtc and Isadtc structure reported in the literature [15-17] were optimized using Gaussian 09W v9.5 [18] with density functional theory (DFT) using Becke 3-parameter (exchange) Lee, Yang and Parr (correlation) hybrid functional (B3LYP) and 6-31G(d,p) basis set in ethanol (solvent) as polarizable continuum model (PCM). The optimized NO_2Isadtc and Isadtc structures were used for infrared calculations using the same level of theory, solvent and basis set from optimization step without anharmonic corrections.

2.4.2. Docking calculations - compound - receptor protocol

In order to have some insights on the drug-receptor binding mode, the molecular docking technique was performed. Human thioredoxin reductase 1 (TrxR) was chosen as the target enzyme. TrxR is known to be a representative target for antitumor drug development [9]. TrxR X-ray crystallographic structure was downloaded from the Protein Data Bank under the code 2J3N [9] and prepared in PyMOL software (https://pymol.org). The homodimer with chains C and D for the docking study was selected. All water molecules were removed and hydrogen atoms were added to the receptor molecule enzyme. Subsequently, molecular docking simulations were performed with the GOLD (Genetic Optimization for Ligand Docking) suit version 5.5 [19] using a receptor-rigid method. Searching for the best complex poses was simulated using 10 Å of radius centered at C498 residue of chain D, which was sufficient to cover all binding cavity. A sequence of 100 genetic algorithm (GA) runs were carried out with 200% of efficiency that generated 100 poses for each of the two compounds (NO_2Isadtc and Isadtc) complexed with TrxR.

Table 1. Crystal data and details of the structure refinement for NO_2Isadtc.

Parameters	NO_2Isadtc
Empirical formula	$C_{16}H_{12}N_4O_3S_2$
Formula weight	372.42
Temperature (K)	293
Crystal system	Triclinic
Space group	$P\bar{1}$
a, (Å)	6.640
b, (Å)	8.256
c, (Å)	15.908
α (°)	80.80
β (°)	80.71
γ (°)	87.91
Volume (Å^3)	849.6
Z	2
ρ_{calc} (g/cm^3)	1.456
μ (mm^{-1})	0.337
F(000)	384
Crystal size (mm^3)	0.12 × 0.59 × 0.74
Radiation	MoKα (λ = 0.71073)
2Θ range for data collection (°)	2.499 to 26.524
Index ranges	$-8 \le h \le 8$, $-10 \le k \le 10$, $-19 \le l \le 19$
Reflections collected	27515
Independent reflections	3518 [R_{int} = 0.0533]
Data/restraints/parameters	3518/0/226
Goodness-of-fit on F^2	1.044
Final *R* indexes [I≥2σ (I)]	R_1 = 0.0367, wR_2 = 0.1006
Final *R* indexes [all data]	R_1 = 0.0398, wR_2 = 0.1045
Largest diff. peak/hole (e Å^{-3})	0.361/-0.285

Table 2. Infrared attributions for experimental and calculated NO_2Isadtc and Isadtc.

Vibration	NO_2Isadtc		Isadtc	
	Calculated (cm^{-1})	Experimental (cm^{-1})	Calculated (cm^{-1})	Experimental (cm^{-1})
ν1A (N-H)	3639, 3401	3595, 3592	3645, 3385	3572, 3489
ν2A (C=O)	1776	1715	1766	1690
ν3A (C=N)	1645	1615	1673	1616
ν4A (C=C)	1503	1529	1649	1492
ν5A (NO_2)	1377	1336	-	-
ν6A (N-N)	1179	1064	1172	1072
ν7A (CSS)	1061	1030	1055	978

Full flexibility of the ligand was permitted and partial flexibility of the protein with diverse solutions generated, ring corners were allowed to flip, conformations were explored, and no constraint applied. ChemScore followed by GoldScore were chosen as the scoring functions of generated poses, as previously described for a metal-based compound bound to TrxR [20]. ChemScore and GoldScore are scoring functions estimated from empirical regression functions with coefficients adjusted to better reproduce the binding energy and binding poses for a set of known testing drug-receptor complexes [21]. The scoring terms are often energy-based, taken as the negative of the sum of the energy terms. Thus, the fitness score is the quantity of interest and the larger the score, the better the compound enzyme pose [22]. The best fitness score pose of the highest-ranking structure of each compound for analysis was chosen. Intermolecular interactions of the best poses were analyzed by using the LigPlot software [23] with the conformational structures presented with PyMOL. The methodologies of the theoretical studies of molecular modeling performed here are similar in manner to previous works [24-27].

3. Results and discussion

3.1. Synthesis and spectroscopic

In Scheme 1, the simplified scheme of NO_2Isadtc preparation is presented. The primary amine group (NH_2) of S-benzyl dithiocarbazate reacts with the non-amidic ketone moiety of 5-nitroisatin, forming the imine bond upon release of a water molecule.

The main IR calculated and experimental attributions of NO_2Isadtc and Isadtc are compared in Table 2. In general, a low difference between the experimental and calculated vibrations is observed. These variations can be attributed to the difference of some bond lengths and angles between both structures, as experimentally, the structure is a solid and the theoretical calculations are performed in a solvent as demonstrated previously and, of course, by the influence of DFT functional and basis set type. Confirmation of the formation of NO_2Isadtc and Isadtc peaks related to ν(C=N) stretching at 1615 cm^{-1} are observed in both structures, which indicates the combination between S-benzyl dithiocarbazide and isatin or 5-nitroisatin. Peaks related to the ν(N-H), ν(C=C), ν(C=O), ν(N-N), and ν(CS) stretching are also observed having the correspondent value also showed in Table 2.

3.2. Structure analysis

In Figure 2, it can be seen that the asymmetric unit of NO_2Isadtc is generated with ORTEP-3 [28] which is the complete molecule with none symmetry operation. According to the crystal data given in Table 1, NO_2Isadtc crystalizes in the triclinic $P\bar{1}$ space group, with a unit cell volume of 849.6 Å^3 and calculated density of 1.456 g/cm^3. The refinement quality was acceptable with wR2 < 0.12, R1 < 0.05, and F^2 (Goodness of fit) between 0.9 and 1.2 as demonstrated in Table 1.

The bond length and angle differences between the calculated and experimental data for NO_2Isadtc are found in Table 3 and a detailed comparison for NO_2Isatc and for Isadtc is found in the supplementary material. The NO_2Isadtc has the bond length medium difference of 0.012 Å (standard deviation of 0.012 Å) and angles a medium of 0.102° (standard deviation of 0.525°) for all non-hydrogen bonds which indicates good correlation between experimental and theoretical structures. Isadtc bond lengths and angles present similar results as NO_2Isadtc, presenting an average bond length difference of 0.013 Å (standard deviation of 0.033 Å) and angle difference medium of 0.219° with a standard deviation of 1.416°.

Table 3. Selected experimental and calculated bond lengths (Å) and angles (°) for NO_2Isadtc.

Bond	Distance (Å)		Atoms	Angle (°)	
	Experimental	Calculated		Experimental	Calculated
C7-N3	1.290	1.295	C7-N3-N4	118.000	117.950
N3-N4	1.342	1.342	N3-N4-C9	119.900	121.440
N4-C9	1.372	1.369	N4-C9-S1	119.000	118.840
C9-S1	1.643	1.669	N4-C9-S2	111.900	112.850
C9-S2	1.742	1.773	S1-C9-S2	129.090	128.310
C1-N1	1.466	1.459	O3-C8-C7	126.500	127.270

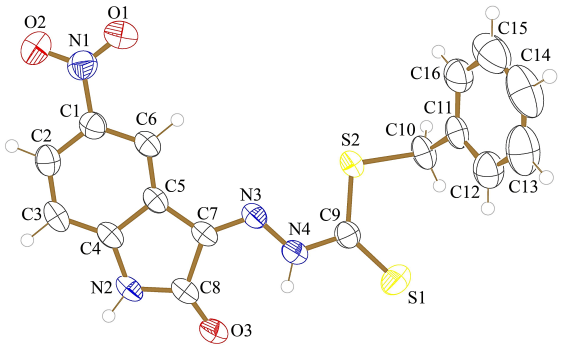

Figure 2. ORTEP plot of the molecular structure of NO_2Isadtc showing thermal ellipsoids at 50% of probability.

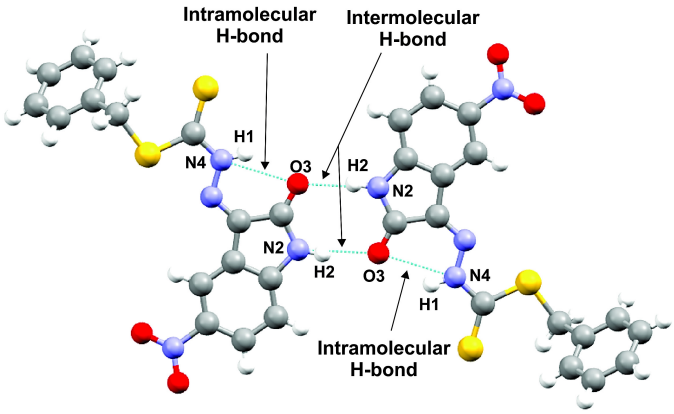

Figure 3. Intra and Intermolecular hydrogen bonds in NO_2Isadtc.

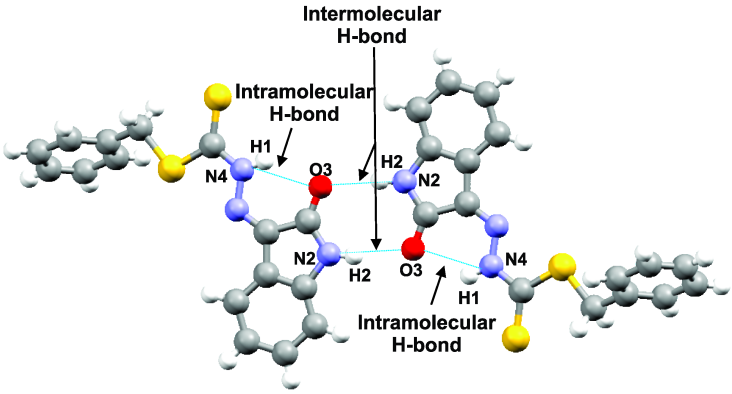

Figure 4. Intra and Intermolecular hydrogen bonds in Isadtc.

The CS bond distances C9-S1 and C9-S2, correspond to double and single bonds, respectively, being in the normal range for other dithiocarbazates [29].

NO_2Isadtc (Figure 3) and Isadtc (Figure 4) present both intramolecular hydrogen bonds between N-H···O atoms with a distance between N4 and O3 of 2.786 Å (angle of 133.6° N4-H1···O3) and 2.788 Å (angle of 133.0° N4-H1···O3) for NO_2Isadtc and Isadtc, respectively. Intermolecular H-bonds also occur with N-H···O atoms with a distance between N2 and O3 of 2.818 Å (angle of 165.3° N2-H2···O3) in NO_2Isadtc and 2.865 Å (angle of 164.4° N2-H2···O3) in Isadtc due the structure similarity.

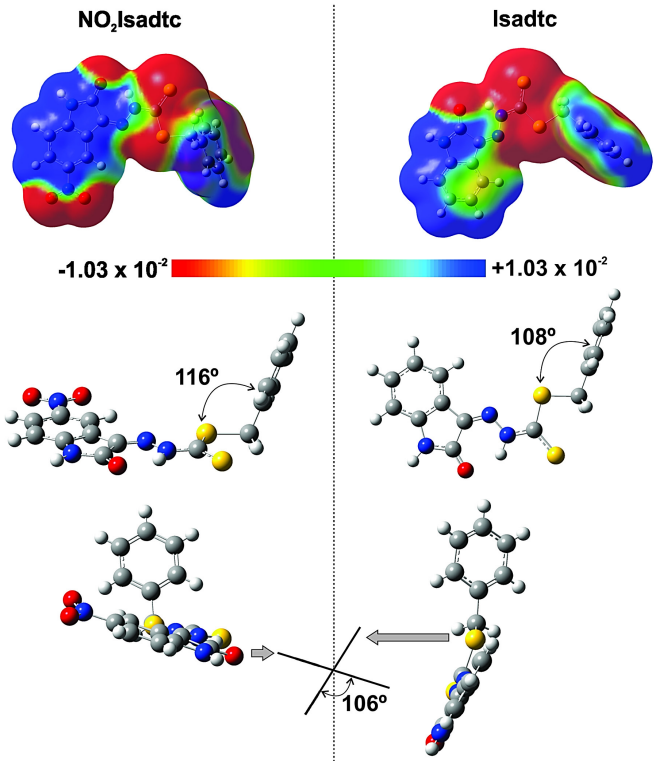

Figure 5. Electrostatic potential and views of NO_2Isadtc and Isadtc.

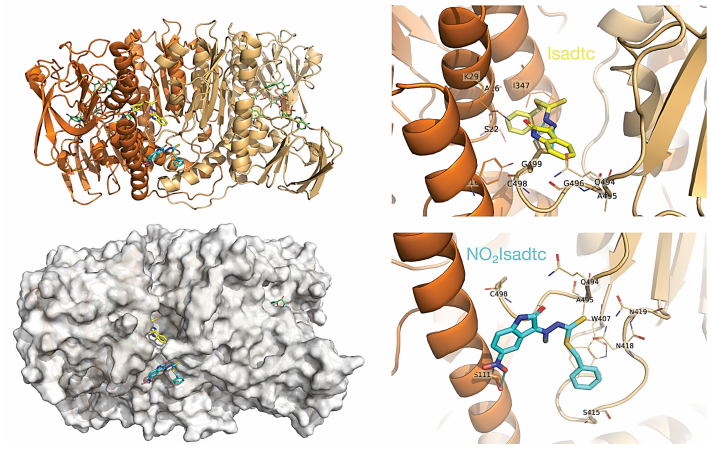

Figure 6. Predicted poses by the docking technique of the human thioredoxin reductase 1 (TrxR) homodimer (light and dark orange) enzyme complexed with NO_2Isadtc (cyan) and Isadtc (yellow) are shown in the same enzyme structure for comparison of the resulted conformations. The TrxR enzyme is shown in a cartoon representation in A) and in a surface representation in C), and the compounds are presented in sticks. In addition, the native enzyme cofactors FAD and $NADP^+$ are shown in green sticks. The enzyme binding site were zoomed in with the docked molecules B) Isadtc and D) NO_2Isadtc, and the enzyme cofactors were removed for better visualization. Side chain residues of the enzyme mediating hydrophobic interactions with Isadtc in B) and NO_2Isadtc in D) are shown in orange lines. Enzyme residues coordinating hydrogen bonds with the compounds, Gly499 in B) and Ser111 in D), are displayed in cyan thin sticks.

Both structures present an angle of approximately 116° and 108° between the phenyl ring and S2 (Figure 5) due the sp^3 carbon C10 helped by the electron repulsion between these planes. A coordination site between O3 and S1 have 4.657 and 4.673 Å of distance in NO_2Isadtc and Isadtc, respectively, being the longest comparing with other possible sites in the same molecules, so the probability of a metal complexation at this site is greater due to the space accommodation and electron density as also demonstrated in Figure 5. It also can be seen that the NO_2 group induces a distortion on the molecule when compared with Isadtc, causing a rotation of approximately 106° on the plane formed by the isatin ring.

3.3. Docking analysis

An *in silico* analysis was performed to better understand the compound receptor binding mode with the human thioredoxin reductase 1 (TrxR) homodimer selected as the target enzyme. The molecular docking technique was used to obtain the geometry of TrxR complexed with the two compounds of this study, NO_2Isadtc and Isadtc. The docked poses are presented in Figure 6, in which NO_2Isadtc and Isadtc are successfully bound at the active redox binding site of TrxR. It is known that TrxR inhibitors might act by coordinating to Cys and Sec residues at the C-terminal active site that is essential for catalysis [20,30,31]. Isadtc resulted in a more buried pose than

NO_2Isadtc that was predicted to be located on the enzyme binding site surface (Figure 6C).

Figure 6 shows that the enzyme compound geometry is stabilized by hydrophobic interactions mediated by residues located in the flexible C-terminal part of one subunit (light orange cartoon) in contact with the other rigid subunit helix (dark orange cartoon). Also, one residue coordinates the hydrogen bond interaction with each compound: G499 at the C-terminal arm with Isadtc (Figure 6B) and S111 at the helix content with NO_2Isadtc (Figure 6D). The binding free energy (ΔG) for the two studied compounds and the enzyme was estimated. ΔG values of -23.2 and -24.1 kcal/mol were obtained for Isadtc and NO_2Isadtc, respectively, estimated by the binding energy function of ChemScore. Similar values for binding ΔG were verified in molecular docking simulations of natural and semisynthetic compounds used in leishmanicidal activity studies [25]. These analyses in the molecular level could bring some insights to future structure-based inhibitor development of antitumor drugs.

4. Conclusion

NO_2Isadtc was successfully synthesized with high yield and had its structure confirmed by IR, NMR and single crystal XRD analysis. Quantum calculations demonstrated that although NO_2Isadtc and Isadtc have similar structures, the first presents an electron density at NO_2 group comparable with the *O-N-S* region, which is responsible for the torsion occurred in the plane formed by the isatin ring. The influence of the electron withdrawing NO_2 group was also verified by docking studies since both NO_2Isadtc and Isadtc can attach to the TrxR enzyme redox site, but Isadtc presents a deeper bind on the enzyme than NO_2Isadtc since the presence of the NO_2 group leads to an interaction with S111 at the helix content. Finally, these results indicate that the insertion of the NO_2 group to the isatin moiety may play a role on the biological activity of isatin derivatives.

Acknowledgements

This work was supported by Conselho Nacional de Desenvolvimento Cientifico e Tecnologico (Grants: 438316/2018-5, 309145/2020-1, 424095/2018-1, 307443/2015-9, 307836/2018-5 and 140219/2020-0), Fundacao de Amparo a Pesquisa de Sao Paulo (Grant 2009/54011-8) and Fundacao de Amparo a Pesquisa do Estado de Minas Gerais (Grants: APQ-00941-14, APQ-03174-18, APQ-01988-14, APQ-00583-13 and APQ-03017-16). This work is also a collaboration research project of members of the Rede Mineira de Quimica and of the Grupo de Materiais Inorganicos do Triangulo-GMIT, research groups supported by Fundacao de Amparo a Pesquisa do Estado de Minas Gerais (Grants: CEX-RED-00010-14 and APQ-00330-14). Computational resources were provided by GridUNESP and CENAPAD-SP.

Supporting information

CCDC-2060140 contains the supplementary crystallographic data for this paper. These data can be obtained free of charge via https://www.ccdc.cam.ac.uk/structures/, or by e-mailing data_request@ccdc.cam.ac.uk, or by contacting The Cambridge Crystallographic Data Centre, 12 Union Road, Cambridge CB2 1EZ, UK; fax: +44(0)1223-336033.

Disclosure statement

Conflict of interests: The authors declare that they have no conflict of interest.
Author contributions: All authors contributed equally to this work.
Ethical approval: All ethical guidelines have been adhered.
Sample availability: Samples of the compounds are available from the author.

Funding

Conselho Nacional de Desenvolvimento Cientifico e Tecnológico (CNPq)
http://www.cnpq.br
Fundação de Amparo a Pesquisa do Estado de Minas Gerais (FAPEMIG)
https://fapemig.br/pt/
Fundação de Amparo a Pesquisa de São Paulo (FAPESP)
http://www.fapesp.br/

ORCID

Pedro Henrique do Nascimento Pereira
https://orcid.org/0000-0003-4146-9617
Jackelinne Camargo Lima
https://orcid.org/0000-0002-2334-5509
Victor Marcelo Deflon
https://orcid.org/0000-0002-5368-6486
Geoffroy Roger Pointer Malpass
https://orcid.org/0000-0002-0036-5750
Ronaldo Junio de Oliveira
https://orcid.org/0000-0003-4860-309X
Pedro Ivo da Silva Maia
https://orcid.org/0000-0003-4699-9481

References

[1]. Silva, B. N. M. da; Bastos, R. S.; Silva, B. V.; Pinto, A. C. *Quim. Nova* **2010**, *33*, 2279–2282.
[2]. Chiyanzu, I.; Hansell, E.; Gut, J.; Rosenthal, P. J.; McKerrow, J. H.; Chibale, K. *Bioorg. Med. Chem. Lett.* **2003**, *13*, 3527–3530.
[3]. Manan, M. A. F. A.; Crouse, K. A.; Tahir, M. I. M.; Rosli, R.; How, F. N.-F.; Watkin, D. J.; Slawin, A. M. Z. *J. Chem. Crystallogr.* **2011**, *41*, 1630–1641.
[4]. El-Sawi, E. A.; Mostafa, T. B.; Radwan, H. A. *Eur. J. Chem.* **2011**, *2*, 539–543.
[5]. Singh, V. P.; Singh, S.; Singh, D. P. *J. Enzyme Inhib. Med. Chem.* **2012**, *27*, 319–329.
[6]. Pavan, F. R.; da S Maia, P. I.; Leite, S. R. A.; Deflon, V. M.; Batista, A. A.; Sato, D. N.; Franzblau, S. G.; Leite, C. Q. F. *Eur. J. Med. Chem.* **2010**, *45*, 1898–1905.
[7]. Singh, R.; Kaushik, N. K. *Main Group Met. Chem.* **2004**, *27* (6), 327–334.
[8]. Yekke-ghasemi, Z.; Takjoo, R.; Ramezani, M.; Mague, J. T. *RSC Adv.* **2018**, *8*, 41795–41809.
[9]. Ramilo-Gomes, F.; Addis, Y.; Tekamo, I.; Cavaco, I.; Campos, D. L.; Pavan, F. R.; Gomes, C. S. B.; Brito, V.; Santos, A. O.; Domingues, F.; Luís, Â.; Marques, M. M.; Pessoa, J. C.; Ferreira, S.; Silvestre, S.; Correia, I. *J. Inorg. Biochem.* **2021**, *216*, 111331.
[10]. Yekke-ghasemi, Z.; Ramezani, M.; Mague, J. T.; Takjoo, R. *New J. Chem.* **2020**, *44*, 8878–8889.
[11]. Fritz-Wolf, K.; Urig, S.; Becker, K. *J. Mol. Biol.* **2007**, *370*, 116–127.
[12]. Maia, P. I. da S.; Fernandes, A. G. de A.; Silva, J. J. N.; Andricopulo, A. D.; Lemos, S. S.; Lang, E. S.; Abram, U.; Deflon, V. M. *J. Inorg. Biochem.* **2010**, *104*, 1276–1282.
[13]. Altomare, A.; Cascarano, G.; Giacovazzo, C.; Guagliardi, A.; Burla, M. C.; Polidori, G.; Camalli, M. *J. Appl. Crystallogr.* **1994**, *27*, 435–435.
[14]. Sheldrick, G. M. *Acta Crystallogr. A* **2008**, *64*, 112–122.
[15]. Abu El-Reash, G. M.; Taha, F.; Shallaby, A. M.; El-Gamal, O. A. *Indian J. Chem., Sect. A: Inorg., Phys., Theor. Anal.* **1991**, *30* (3), 286-289. http://nopr.niscair.res.in/handle/123456789/41831 (accessed April 6, 2021).
[16]. Ali, M. A.; Mirza, A. H.; Bakar, H. J. H. A.; Bernhardt, P. V. *Polyhedron* **2011**, *30*, 556–564.
[17]. Xia, J.-J. *J. Struct. Chem.* **2014**, *55*, 130–133.
[18]. Frisch, M. J.; Trucks G. W.; Schlegel, H. B.; Scuseria, G. E.; Robb, M. A.; Cheeseman, J. R.; Scalmani, G.; Barone, V.; Mennucci, B.; Petersson, G. A.; Nakatsuji, H.; Caricato, M.; Li, X.; Hratchian, H. P.; Izmaylov, A. F.; Bloino, J.; Zheng, G.; Sonnenberg, J. L.; Hada, M.; Ehara, M.; Toyota, K.; Fukuda, R.; Hasegawa, J.; Ishida, M.; Nakajima, T.; Honda, Y.; Kitao, O.; Nakai, H.; Vreven, T.; Montgomery, J. A.; Peralta, J. E.; Ogliaro, F.; Bearpark, M.; Heyd, J. J.; Brothers, E.; Kudin, K. N.; Staroverov, V. N.; Kobayashi, R.; Normand, J.; Raghavachari, K.; Rendell, A.; Burant, J. C.; Iyengar, S. S.; Tomasi, J.; Cossi, M.; Rega, N.; Millam, J. M.; Klene, M.;

Knox, J. E.; Cross, J. B.; Bakken, V.; Adamo, C.; Jaramillo, J.; Gomperts, R.; Stratmann, R. E.; Yazyev, O.; A. J. Austin, A. J.; Cammi, R.; Pomelli, C.; Ochterski, J. W.; Martin, R. L.; Morokuma, K.; Zakrzewski, V. G; Voth, G. A.; Salvador, P.; Dannenberg, J. J.; Dapprich, S.; Daniels, A. D.; Farkas, O.; Foresman, J. B.; Ortiz, J. V.; Cioslowski, J.; Fox, D. J. Gaussian, Inc. , Gaussian 09, Revision D.01-SMP, Wallingford CT, 2013.

[19]. Jones, G.; Willett, P.; Glen, R. C.; Leach, A. R.; Taylor, R. *J. Mol. Biol.* **1997**, *267*, 727–748.

[20]. Tavares, T. T.; Azevedo, G. C.; Garcia, A.; Carpanez, A. G.; Lewer, P. M.; Paschoal, D.; Müller, B. L.; Dos Santos, H. F.; Matos, R. C.; Silva, H.; Grazul, R. M.; Fontes, A. P. S. *Polyhedron* **2017**, *132*, 95–104.

[21]. Verdonk, M. L.; Cole, J. C.; Hartshorn, M. J.; Murray, C. W.; Taylor, R. D. *Proteins* **2003**, *52*, 609–623.

[22]. Meng, X.-Y.; Zhang, H.-X.; Mezei, M.; Cui, M. *Curr. Comput. Aided Drug Des.* **2011**, *7*, 146–157.

[23]. Laskowski, R. A.; Swindells, M. B. *J. Chem. Inf. Model.* **2011**, *51*, 2778–2786.

[24]. Gonçalves, A. C. R.; Carneiro, Z. A.; Oliveira, C. G.; Danuello, A.; Guerra, W.; Oliveira, R. J.; Ferreira, F. B.; Veloso-Silva, L. L. W.; Batista, F. A. H.; Borges, J. C.; de Albuquerque, S.; Deflon, V. M.; Maia, P. I. S. *Eur. J. Med. Chem.* **2017**, *141*, 615–631.

[25]. Lacerda, R. B. M.; Freitas, T. R.; Martins, M. M.; Teixeira, T. L.; da Silva, C. V.; Candido, P. A.; Oliveira, R. J. de; Júnior, C. V.; Bolzani, V. da S.; Danuello, A.; Pivatto, M. *Bioorg. Med. Chem.* **2018**, *26*, 5816–5823.

[26]. Lopes, C. D.; Possato, B.; Gaspari, A. P. S.; Oliveira, R. J.; Abram, U.; Almeida, J. P. A.; Rocho, F. dos R.; Leitão, A.; Montanari, C. A.; Maia, P. I. S.; da Silva, J. S.; de Albuquerque, S.; Carneiro, Z. A. *ACS Infect. Dis.* **2019**, *5*, 1698–1707.

[27]. Sousa, L. M.; Souza, W. A.; Paixão, D. A.; Fazzi, R. B.; Tezuka, D. Y.; Lopes, C. D.; Carneiro, Z. A.; Moreira, M. B.; Pivatto, M.; Netto, A. V. G.; de Albuquerque, S.; Ferreira, F. B.; De Oliveira, R. J.; Resende, J. A. L. C.; Lino, R. C.; De Oliveira Júnior, R. J.; Da Costa Ferreira, A. M.; Guerra, W. *Inorg. Chim. Acta* **2020**, *511*, 119824.

[28]. Farrugia, L. J. *J. Appl. Crystallogr.* **1997**, *30*, 565–565.

[29]. Carneiro, Z. A.; Lima, J. C.; Lopes, C. D.; Gaspari, A. P. S.; de Albuquerque, S.; Dinelli, L. R.; Veloso-Silva, L. L. W.; Paganelli, M. O.; Libardi, S. H.; Oliveira, C. G.; Deflon, V. M.; Oliveira, R. J.; Borges, J. C.; Maia, P. I. S. *Eur. J. Med. Chem.* **2019**, *180*, 213–223.

[30]. Ilari, A.; Baiocco, P.; Messori, L.; Fiorillo, A.; Boffi, A.; Gramiccia, M.; Di Muccio, T.; Colotti, G. *Amino Acids* **2012**, *42*, 803–811.

[31]. Messori, L.; Scaletti, F.; Massai, L.; Cinellu, M. A.; Gabbiani, C.; Vergara, A.; Merlino, A. *Chem. Commun. (Camb.)* **2013**, *49*, 10100–10102.